Journal of Applied Polymer Science

Joining of carbon fiber reinforced polymer laminates by a novel partial cross-linking process

Judith Moosburger-Will,[1] Markus G. R. Sause,[1] Robert Horny,[1] Siegfried Horn,[1] Jochen Scholler,[2] Llorenç Llopard Prieto[2]

[1]Experimental Physics II, Institute of Physics, University of Augsburg, 86135 Augsburg, Germany

[2]Premium AEROTEC GmbH, 86179 Augsburg, Germany

Correspondence to: J. Moosburger-Will (E-mail: judith.will@physik.uni-augsburg.de)

ABSTRACT: Direct joining of partially cross-linked and freshly infiltrated carbon fiber reinforced epoxy resin plates made from HTA/RTM6 is investigated as function of the partial curing degree. Partial cross-linking maintains a certain chemical reactivity of the thermosetting resin which can be used for bonding to a second, freshly infiltrated resin part. A final curing cycle guarantees complete cross-linking of the joined component. The bonding behavior and the interface morphology of the joined plates are analyzed by mechanical testing, acoustic emission analysis and microscopy. A significant dependence of the bonding and interfacial properties on the partial curing degree is found. Very low and very high partial curing degrees (below 70% and above 80%) result in low fracture toughness and discontinuous crack propagation. Intermediate curing degrees between 70% and 80% mainly show high fracture toughness, stable crack propagation and a ripple like interface morphology. The latter is created by the surface morphology of the partially cross-linked plate with the typical peel-ply imprint and results in a high contact surface and mechanical interlocking. The combination of chemical reactivity and high contact surface seems to be advantageous for the enhanced fracture toughness and the improved failure mode of samples with intermediate partial curing degree. © 2015 Wiley Periodicals, Inc. J. Appl. Polym. Sci. **2015**, *132*, 42159.

KEYWORDS: composites; crosslinking; surfaces and interfaces; thermosets

Received 23 December 2014; accepted 2 March 2015

DOI: 10.1002/app.42159

INTRODUCTION

The high lightweight potential and the extraordinary specific mechanical properties of carbon fiber reinforced polymers (CFRP) are responsible for their growing importance in aerospace and automotive industry. Due to superior thermo-mechanical properties, tetra-functional epoxy resins are widely used as matrix materials.[1–3] For broader industrial application, joining of composite components is of high relevance to achieve an increased level of integral construction. Commonly, joining of thermosetting composite parts is done by mechanical fastening with metallic bolts or blanks or by adhesive bonding.[4,5] However, the correspondent insertion of different materials and the creation of additional interfaces can be problematic and needs thorough processing. Mechanical fastening involves the drilling of holes in the CFRP material. One major problem is the stress concentration in the CFRP due to the presence of these holes and possible preliminary damage due to the drilling process. Besides, the direct contact of metal bolts or blanks and the conductive carbon fibers can cause contact corrosion of the metallic parts.[6] Use of metals with a high standard electrode potential similar to that of graphite or use of insulating interfacial layers is necessary.[5,7]

Use of an adhesive layer also causes a discontinuity of the material properties, which results in an abrupt change of the stiffness. Bonding between adhesive and adherent is determined by different adhesion mechanisms, namely mechanical interlocking, chemical and physical bonding (adsorption interaction), electrostatic forces and diffusion mechanisms.[8,9] Therefore, the properties of the joining depend sensitively on the specific material properties of the used adhesive and the surface properties of the adherents. In particular the surface roughness, the wetting properties and the chemical compositions are of substantial influence. Thorough surface preparation is indispensable before application of the adhesive and joining of the components. An increase of surface area is achieved by the use of peel-ply textiles or grid blastening. A modification of the chemical composition of the surface is done e.g. by plasma treatment.[4,10,11] Besides, adhesive bonds may fail at low loads due to crack opening modes and the adhesive properties may suffer from thermal and environmental degradation.[5]

An alternative joining concept for thermosetting CFRP components is based on direct bonding of partly cross-linked and fresh resin parts.[12] The same resin system, in our case the tetra-

functional epoxy resin system HexFlow® RTM6, is used for both components. No additional materials as metallic parts or adhesives are used, avoiding the mentioned problems of common joining methods. Partial cross-linking can be achieved by a thermal curing treatment at reduced temperatures and/or reduced curing times.[13] It maintains a particular reactivity of the thermosetting resin, as a reduced extent of polymer and hardener molecules are cross-linked. A chemical reaction of unreacted functional groups with the fresh resin of the second CFRP part is possible and can be used for joining of the partially cured and the fresh component. A final curing cycle of the joined parts guarantees complete cross-linking of the final component.

For low and intermediate partial curing degrees (below 80%) and correspondingly low glass transition temperatures (below 150°C) of the partially cross-linked plate, the final curing cycle results in a softening of the polymer. A particular intermixture of softened and fresh resin becomes possible. Besides, the use of peel-ply materials allows a modification of the CFRP surface roughness of the partially cured plate and enables additional mechanical interlocking of the joined parts. The morphology of the surface is influenced by the adhesion between resin and peel-ply,[11] namely the resulting pull-off properties, which in turn can be affected by the cross-linking degree.

The alternative joining concept thus combines three different adhesion mechanisms: chemical reactivity of CFRP surface and bulk material, diffusion effects between fresh and partially cured resin and mechanical interlocking of the joined CFRP parts.

In order to quantify the interlaminar joint strength, mode I fracture mechanics experiments are established as testing method. For this purpose, double cantilever beam (DCB) tests as recommended by ASTM D 5528 are typically used. In order to allow a correlation between mechanical properties and microscopic processes, acoustic emission (AE) signals can be recorded during the experiment[1–4,18] The microscopic failure mechanisms of interest are fiber breakage, matrix cracking and all sorts of interfacial failure occurring between fiber and matrix (i.e. fiber-matrix debonding, fiber pull-out). Since each of these microscopic failure mechanisms is accompanied by acoustic emission, the detection of the signals at the surface of the solid and their analysis forms a powerful tool to investigate interlaminar failure.

In the present work a mechanical and microscopic analysis of joined partially cross-linked and freshly infiltrated CFRP components is done. The fracture toughness of the joined plates and the acoustic emission activity during mechanical testing are investigated as function of the partial curing degree. Additionally, the surface morphology of the first plate, the structure of the interface region between first and second plate before mechanical testing and the morphology of the fracture surface after mechanical testing are analyzed by microscopic methods.

EXPERIMENTAL

Joining of Partially Cross-Linked CFRP Plates

All CFRP samples analyzed in this work use the high tenacity carbon fibers Tenax® HTA 40, distributed by the Toho Tenax Europe GmbH.[5] As polymeric matrix material the monocomponent epoxy resin system HexFlow® RTM6, distributed by the Hexcel Corporation, is used.[6] It is composed of the tetrafunctional epoxy resin Tetraglycidyl Methylene Dianiline (TGMDA) and the hardeners 4,4'-Methylenebis(2,6-diethylaniline) (MDEA) and 4,4'-Methylenebis(2-Isopropyl-6-methylaniline) (M-MIPA).[13,20] All HTA/RTM6 specimens were manufactured in a vacuum assisted resin infusion process using the VAP®-technique. The applied vacuum draws the liquid, thermosetting resin through the dry fiber fabric and impregnates it. The VAP®-technique utilizes semi-permeable membrane systems to apply the effect of vacuum to the entire surface of the component and to effectively remove air and gas. The peel-ply textile WELA T0098 is used to assist in the VAP process.

A two-stage infiltration and curing process is used. In a first step a partially cross-linked CFRP plate is produced. In our previous work the modified curing cycles, which are used to obtain defined partial curing degrees of the RTM6 resin system, are described in detail.[13] All cycles start with an isothermal curing period at a temperature of 120°C, technically used as infiltration cycle. To create a completely cross-linked sample with a curing degree of nearly 100% the resin is cured subsequently for 2.5 h at a heating temperature of 180°C. To obtain samples with partial curing degrees between 55% and 80% the infiltration cycle is followed by isothermal heat treatment at a reduced temperature of 135°C. The different curing degrees result from different durations of these isothermal heating periods. As fiber reinforcement of this first plate unidirectional carbon fiber layers with stacking sequence (0/90)(0/90)(90/0)(90/0) are used.

In a second step, on top of the first, partially cross-linked CFRP plate a second, dry fiber fabric of same stacking sequence is positioned and infiltrated with fresh RTM6 epoxy resin. At the medial plane of the specimens a folded Polytetrafluoroethylene (Teflon) stripe with 13 μm thickness is inserted, to provide an initiation site of 50 mm length for delamination during mechanical testing. For final curing, this combination of partially cross-linked and fresh carbon fiber reinforced polymer is submitted to a second curing cycle at 180°C for 2.5 h. The second curing step transforms the partially cross-linked resin, e.g., with a curing degree of 60%, to a completely cross-linked resin further nominated as "60/100". The fresh resin system is completely cross-linked to a curing degree of about 100%. The resulting joined CFRP plate thus is composed of a lower 60/100-part and an upper 100-part and in the following is named "60/100-100". The other curing degrees investigated are referred to, respectively. The joined plates have a thickness of (5.7 ± 0.2) mm.

Additionally, a reference CFRP plate with the same stacking sequence as the joined CFRP plates is produced, which is infiltrated in one step and is completely cured to a curing degree of about 100%. This plate is named "100ref" and also has a thickness of (5.7 ± 0.2) mm.

Mode-I Interlaminar Fracture Toughness and Acoustic Emission Analysis

The mode-I interlaminar fracture toughness values were measured in a load frame according to ASTM D 5528. Double cantilever beam specimens with dimensions of (250 ± 2) mm ×

(25 ± 0.2) mm $\times$ (5.7 ± 0.2) mm (length $\times$ width $\times$ height) were tested using an universal testing machine with a 5 kN load cell. The crosshead speed was set to 5 mm/min to create an effective crack length of 100 mm length.

During the measurement two multi-resonant acoustic emission sensors (type WD) were mounted using medium viscosity silicone grease. Signals were acquired using a preamplifier with 40dB$_{AE}$ gain, and an acquisition card with 10 MSP/s acquisition rate (type PCI-2). Signal detection was carried out in triggered mode using 35 dB$_{AE}$ threshold level and 10 µs Peak-Definition-Time, 80 µs Hit-Definition-Time and 300 µs Hit-Lockout-Time. To obtain acoustic emission source positions a localization procedure using the delta-t method was used.

For each type of joined samples, i.e., for each curing degree, four samples were analyzed.

Microscopic Analysis of Crack Area and Cross Section

Microscopic analyses of CFRP cross sections and fracture surfaces after mechanical testing were performed by digital optical microscopy (Keyence GmbH, VHX-100) and environmental scanning electron microscopy (FEI company, XL30). Cross-sections of the joined CFRP plates were prepared by a grinding and polishing process.

Micromechanical modulus determination was done by scanning probe measurements (Veeco, Dimension Icon Scanning Probe Microscope) in the Peak Force Quantitative Nano Mechanics mode. Height images and quantitative nanomechanical sample property images are measured simultaneously. A detailed description of the method and the used experimental setup is included in our previous work.[21]

RESULTS AND DISCUSSION

In the following the bonding and failure behavior of joined partially cured CFRP plates is analyzed by mechanical testing, acoustic emission analysis and microscopic analysis of CFRP cross sections and crack surfaces after mechanical testing. The influence of the partial curing degree of the first CFRP plate on the mechanical properties and the interface morphology of the joined plate are addressed.

Determination of Mode-I Interlaminar Fracture Toughness

In general, the mode-I interlaminar fracture toughness value can be used to analyze the bonding quality of joined CFRP plates. Usually travelling microscopes or high resolution camera systems are used to follow the position of the crack tip during mechanical loading. The progress of delamination is then obtained via measurement of the crack progress between subsequent images. Using the delamination length as a function of loading it is thus possible to calculate the delamination resistance curve (R-curve), which represents the strain energy release rate G_I as function of delamination length a. However, the number of images evaluated for delamination lengths is usually limited, since this involves manual processing of each image. In the present study we use acoustic emission source localization to track the position of the crack tip during mode-I tests. This approach follows previous investigations by Refs. 1, 2, and 16

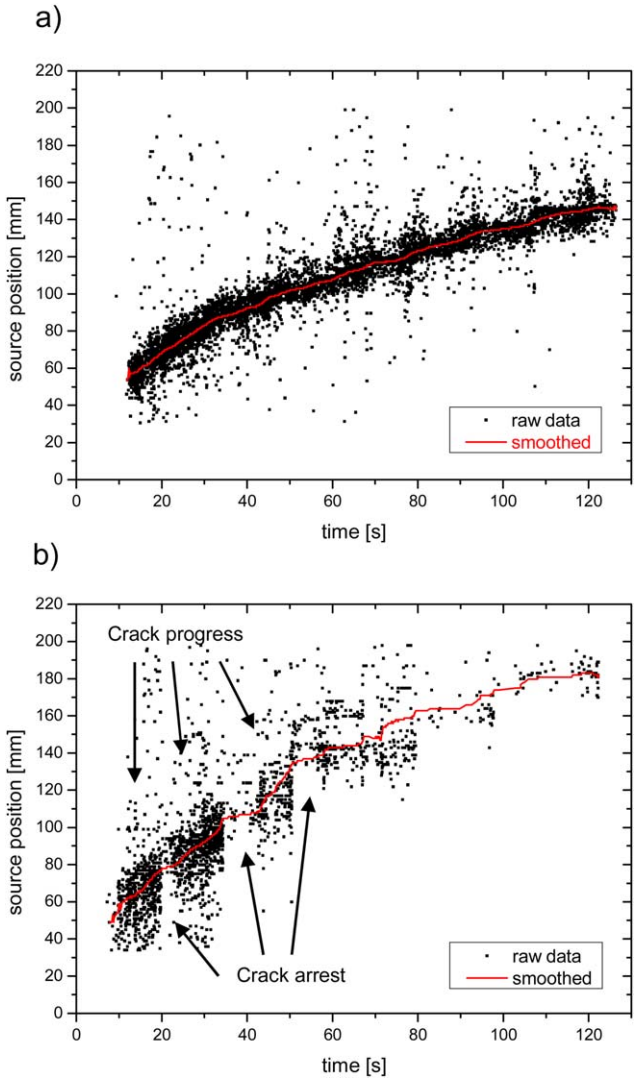

Figure 1. Acoustic emission source positions during DCB test of (a) one reference sample 100ref and (b) one sample 100/100 as function of time. Exemplary the regions of crack progress and crack arrest are marked. [Color figure can be viewed in the online issue, which is available at wileyonlinelibrary.com.]

and can be used to generate continuous R-curves, as will be demonstrated in the following.

In Figure 1(a) the result from a DCB measurement of one of the 100ref reference specimens is shown. Acoustic emission signals were localized in one dimension between the two sensors and are shown as function of time. Each data point represents one acoustic emission signal; the number of signals per time is called acoustic emission activity. During the whole period of mechanical testing distinct acoustic emission activity and continuous crack propagation is observed. In order to obtain an effective crack length as function of time, the raw data was smoothed using a percentile filter with 1500 points window size. Compared to other averaging techniques (adjacent averaging, Savitzky-Golay method) this filter is less affected by outliers and better reflects the achieved crack length. In particular for those cases with crack arrest, steps in the delamination length

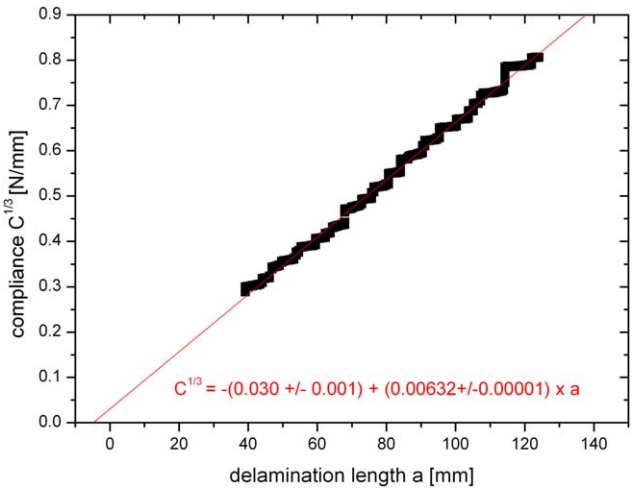

Figure 2. Compliance data of one reference sample 100ref and linear fit to obtain shift of effective delamination length Δ. [Color figure can be viewed in the online issue, which is available at wileyonlinelibrary.com.]

occur. The percentile filter is able to preserve these jumps and therefore resembles a reasonable method to obtain effective crack lengths of the damage zone surrounding the crack tip. For comparison, the result of a 100/100-100 specimen is shown in Figure 1(b). Here the crack propagation is observed to be discontinuous and therefore, the acoustic emission signals are mainly detected at times of active crack progress. During times of crack arrest very low acoustic emission activity is found. This translates into the step-like progression of the so obtained effective crack length.

Using an interpolation scheme of the smoothed AE source position it is possible to obtain a continuous representation of the delamination length a. In combination with the recorded force P, the cross-head displacement δ and specimen width b this allows for calculation of the strain energy release rate G_I using the modified beam theory method [ASTMD5528]:

$$G_I = \frac{3P\delta}{2b(a+|\Delta|)} \quad (1)$$

According to ASTM D 5528, the offset value Δ is obtained from a linear fit of the measured compliance ($C = \delta/P$) to the power of 1/3 as a function of delamination length as shown in Figure 2. For those specimens exhibiting crack arrests only the initial slope (i.e. the range free of crack arrests) was used for the linear fit procedure.

Evaluation of eq. (1) results in the continuous *R*-Curve shown in Figure 3. Using the onset of acoustic emission it is possible to define a measure for the onset of crack growth. During the experiments it was observed, that this definition for the crack onset precedes the visible crack onset and can thus be understood as conservative estimation for G_{Ic}.

For the reference sample 100ref_6 (*R*-Curve shown in Figure 3) the minimum value of the strain energy release rate at the onset of acoustic emission (in the following called G_{Ic}), i.e. the G_I value at crack onset, can be determined as 268.7 J/m^2. Accordingly it is feasible to define a mean G_I value during crack propagation ($G_{I,mean}$) as arithmetic average of all values. For sample 100ref_6 this mean G_I value amounts to 305.6 J/m^2. Compared to the G_{Ic} value of pure RTM-6 resin of 168 J/m^2 the measured onset and mean propagation values are substantially higher.

Fracture Surface Morphology After Fracture Toughness Testing

In the following the correlation between the fracture morphology and the measured *R*-curves is discussed. For the reference sample 100ref distinct acoustic emission activity is observed after crack onset [see Figure 1(a)]. The signal activity is more or less constant for the duration of crack growth. The sample thus is characterized by continuous crack propagation. Besides, the absolute number of acoustic emission signals is relatively high during the whole test, which is characteristic for a continuously high number of microscopic failure processes. This is typical for unidirectional specimens and thus yields an effective mechanism to absorb energy during crack progress.

The electron microscopy image of the fracture surface, shown in Figure 4(a), underlines this interpretation. The surface morphology is dominated by fiber rich regions, which show the unidirectional fiber geometry of the fabric layers [see Figure 4(a), right part]. Only rarely matrix regions with a smooth crack surface exist on the fracture surface, e.g., in the lower left part of Figure 4(a). This fiber dominated fracture morphology points to a high extent of interlaminar splitting and fiber breakage within the unidirectional layer, which are both known as energy absorbing failure modes. The fibrous structures, which run in horizontal direction, are the polymeric sewing threads of the non-crimp fabric or their imprints and will not be considered in the following.

In Figure 5 the *R*-curve of a sample with low fracture toughness is shown. In total the 100/100-100 samples were found to have the lowest average fracture toughness of all analyzed specimens. The G_{Ic} value of the individual sample shown (sample 100/100-100_2) amounts to 109.7 J/m^2, its mean G_I value during crack propagation amounts to 81.7 J/m^2. After crack initiation the

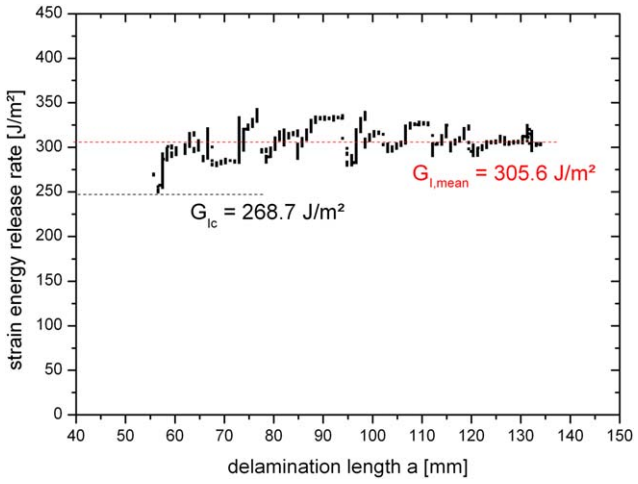

Figure 3. *R*-curve of reference sample 100ref_6 including G_{Ic} and $G_{I,mean}$ value. [Color figure can be viewed in the online issue, which is available at wileyonlinelibrary.com.]

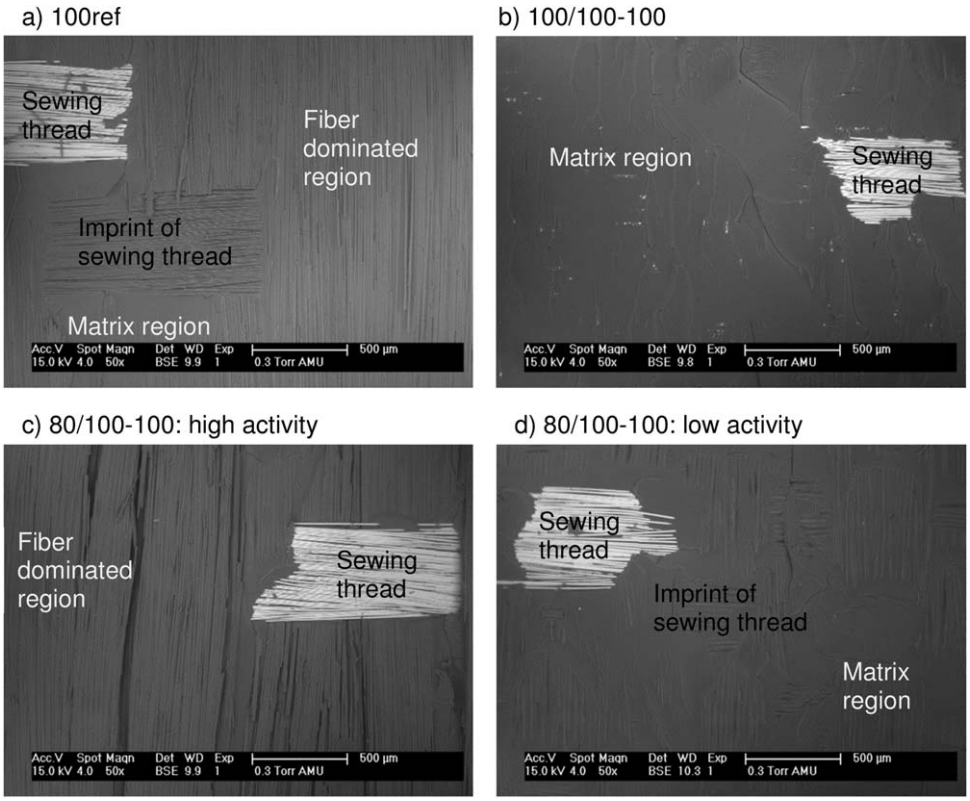

Figure 4. Fracture surfaces of DCB specimen after mechanical testing: (a) reference sample, (b) 100/100-100 sample, (c) and (d) regions of 80/100-100 with high and low acoustic emission activity.

recorded acoustic emission activity is very low compared to that of the reference samples [see Figure 1(b)]. Additionally, a discontinuous crack growth is observed. For the present example, three subsequent sudden jumps of the strain energy release rate are easily identifiable in the *R*-curve at 72 mm, 96 mm, and 126 mm delamination length. Before sudden G_I release, the G_I values increase slowly until reaching a maximum. Therefore, the overall failure of these samples during G_{Ic}-testing can be characterized as discontinuous crack propagation, where regions of stable crack growth and regions of crack arrest alternate. The microscopic analysis of the crack surface [Figure 4(b)] reveals a very smooth morphology with almost pure matrix cracking. Almost no interlaminar splitting or fiber breakage are observed. Also for the other type of joined partially cross-linked samples with low fracture toughness values, namely the 60/100-100

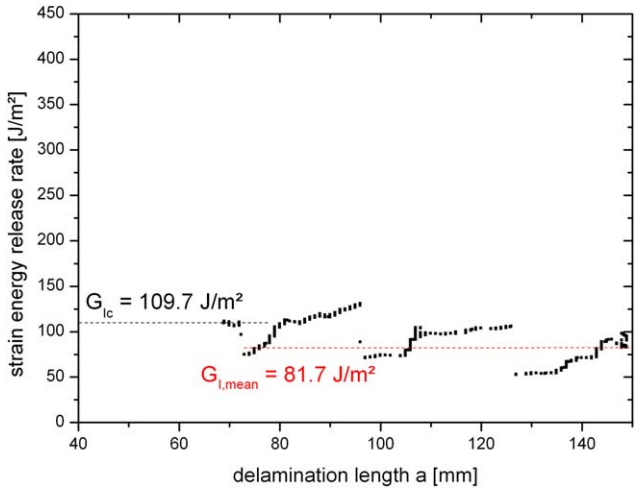

Figure 5. *R*-curve of reference sample 100/100-100_2 including G_{Ic} and $G_{I,mean}$ value. [Color figure can be viewed in the online issue, which is available at wileyonlinelibrary.com.]

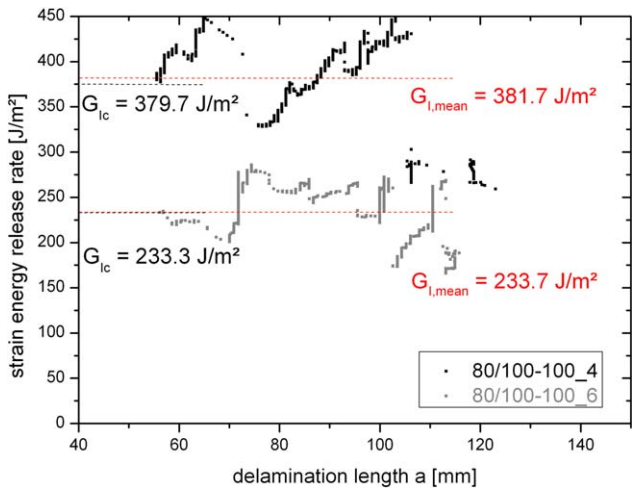

Figure 6. *R*-curves of samples 80/100-100_4 and 80/100-100_6 including G_{Ic} and $G_{I,mean}$ values. [Color figure can be viewed in the online issue, which is available at wileyonlinelibrary.com.]

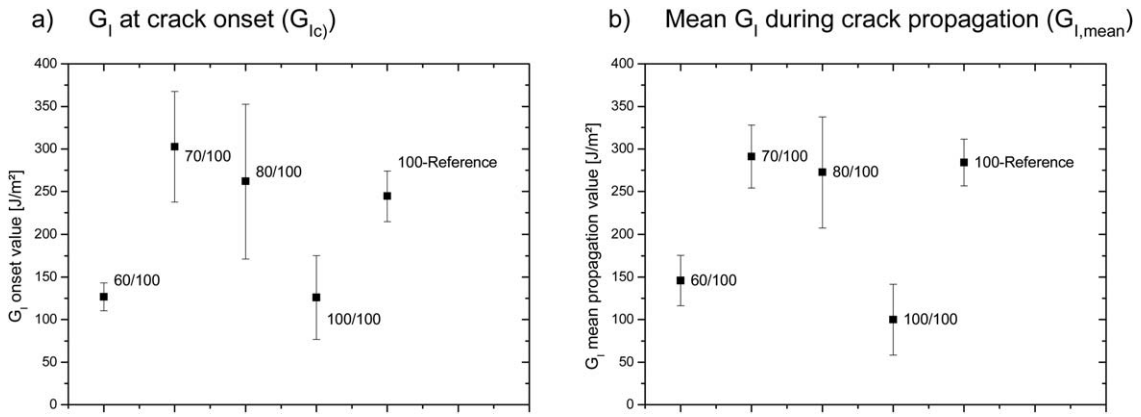

Figure 7. Mode-I interlaminar fracture toughness values of four types of joined CFRP plates and the reference samples: (a) at first crack onset and (b) mean values during crack propagation.

specimens, similar discontinuous crack growth and smooth fracture surfaces are found.

For the samples of type 80/100-100 no consistent bonding behavior was observed. In Figure 6 the *R*-curves of two individual samples of this type are shown, which differ clearly in their fracture toughness values. For one of the samples of type 80/100-100, the sample 80/100-100_4, extraordinary high strain energy release rates were observed. Their G_{Ic} value of 379.7J/m^2 exceeds the typical G_{Ic} values of the reference samples 100ref. Also $G_{I,mean}$ is found at a clearly higher level of 381.7 J/m^2. Other samples of type 80/100-100, e.g., sample 80/100-100_6, exhibit comparatively small values. Here G_{Ic} amounts to only 233.3J/m^2, the mean G_I to 233.7J/m^2.

Also the fracture surface morphology indicates a distinct difference between the two individual samples. The sample with high fracture toughness is characterized by a fiber dominated, quite rough fracture surface with interlaminar splitting and fiber breakage, as exemplary shown in Figure 4(c). In accordance, high acoustic emission activity is found, indicating crack propagation with a high number of energy absorbing microscopic failure processes.

The sample with lower G_{Ic} values shows a relatively smooth fracture surface, as shown in Figure 4(d). It is dominated by regions of pure matrix cracking, accompanied by only a minor amount of fiber dominated regions. Low acoustic emission activity is found, characterized by a high number of regions with negligible acoustic emission activity, followed by regions with relatively low intensity. This translates into a *R*-curve at lower level exhibiting some sudden jumps of G_I.

Figure 7 presents a summary of the measured mode-I interlaminar fracture toughness values of all four types of joined CFRP plates with different partial curing degrees. For comparison also the values of the reference sample are reported. Figure 7(a) shows the G_I values obtained for the first crack onset (G_{Ic}) and Figure 7(b) shows the mean G_I values obtained during crack propagation ($G_{I,mean}$). All values are reported as average values of the measurement series including the standard deviation of the measurement series.

The reference sample 100ref shows high G_I values, both for the first crack onset (244.5 J/m^2 ± 29.4 J/m^2) and during crack propagation (284.0 J/m^2 ± 27.5 J/m^2). Here the infiltration and curing was done in one step, no real joining of plates exists. The properties thus correspond to the interlaminar bonding of the stacked fiber layers of a conventionally manufactured, completely cured CFRP plate and define the G_I values for optimal bonding.

For the joined plates with different partial curing degrees of the first part, clear differences of fracture toughness are observed. Joining of a completely cured CFRP plate with the freshly infiltrated resin part (100/100-100 sample) results in the lowest fracture toughness values, both at crack onset (125.9 J/m^2 ± 49.3 J/m^2) and during crack propagation (100.1 J/m^2 ± 41.7 J/m^2). Very low curing degrees of the partially cured plate of 60% result in similar, small G_I values at crack onset (126.7 J/m^2 ± 16.3 J/m^2) and in average (145.8 J/m^2 ± 29.7 J/m^2). Highest bonding of the joined CFRP plates is achieved for partial curing degrees of the first plate of 70 and 80%. The 70/100-100 sample exhibits the highest fracture toughness at onset (302.6 J/m^2 ± 64.8 J/m^2) and during crack propagation (291.1 J/m^2 ± 36.9 J/m^2). The G_I values are even above that of the reference sample. The fracture toughness values of the 80/100-100 specimens are of similar dimensions (262.0 J/m^2 ± 90.8 J/m^2 and 272.7 J/m^2 ± 65.0 J/m^2). However, within the series of type 80/100-100 a very high variance of the G_I single values is found, both for crack onset and for crack propagation, which might result from differences of the failure behavior.

Surface Morphology of Partially Cured Plates Prior to Joining

Clear differences are observed in the fracture toughness, the crack propagation and the morphology of the fracture surface of the joined samples with different partial cross-linking degrees. To elucidate the reasons for these different material properties, the surface morphology of the first, partially cross-linked plate before joining is of interest. Cross sections of the surface region of the first plate were prepared, to investigate the resin morphology. In Figure 8 the cross sections of the four different types of plates with curing degrees of 60, 70, 80, and 100% are shown. The different orientation of the topmost fiber layer results from different orientation of the prepared cross section surface and can be neglected in the following.

During CFRP production via VAP® the surface of the component is covered with a textile peel-ply material. After the curing

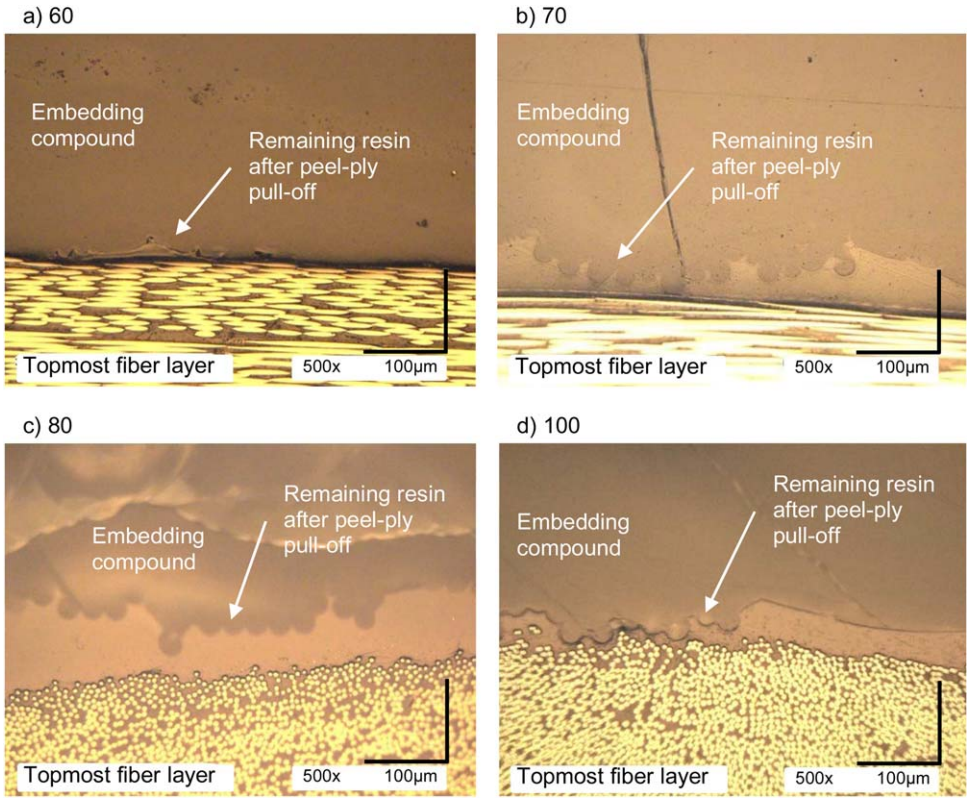

Figure 8. Cross section images of surface region of CFRP plates before joining: plates with curing degree of (a) 60%, (b) 70%, (c) 80%, and (d) 100%. [Color figure can be viewed in the online issue, which is available at wileyonlinelibrary.com.]

procedure, the peel-ply is pulled off. If a complete peeling without resin adhesion is possible, the imprint of the textile with a regular, ripple like pattern defines the residual surface morphology. If the adhesion between textile and resin is high and/or the mechanical properties of the resin are low, the outermost resin layer breaks and is partly removed. Smooth surface regions of cohesively failed resin are the result.

For very low curing degrees of about 60%, a considerable amount of resin of the outermost layer is removed by the peel-ply pull-off [see Figure 8(a)]. The remaining surface shows large zones of cohesively failed resin, which are relatively smooth. Only small regions with minor ripple-like structure exist. For this low partial curing degree, the cross-linking density of the thermosetting resin is quite low. Therefore, the resin has a low mechanical stability and exhibits a very brittle failure behavior.[7] Hence, the adhesion to the peel-ply can cause significant cohesive failure.

In contrast, CFRP plates with partial curing degrees of 70 and 80% show pronounced ripple like structures on a majority of the surface region [see Figure 8(b,c)]. Nearly no cohesive failure of the resin is found. For these curing degrees the resin exhibits improved mechanical properties. High modulus and density values of the pure resin and high resin dominated mechanical properties of the corresponding CFRP plates are reported.[7,13] Therefore, the resin material withstands the peel-ply pull-off very well and an adhesive separation of peel-ply and resin is possible. A rough, periodically structured surface of the CFRP plate with a high effective surface area is created, which is likely advantageous for bonding to a second plate.

For the completely cured CFRP plate with curing degree of nearly 100%, regions with ripple like structure and smooth regions with ruptured resin are found, as shown in Figure 8(d). Compared with the 80% curing degree, lower mechanical properties and a lower density are observed, which may result in the increased amount of cohesive failure.[7,13]

Interface Morphology of the Joined Double Cantilever Beam Samples Prior to Mechanical Testing

To understand the differences in the fracture toughness of the joined samples with different partial cross-linking degrees, also the morphology of the interface region of the double cantilever beam samples prior to mechanical testing is of interest. Therefore, a microscopic investigation of cross sections of the interface region of the joined samples is done.

During the joining process, the fresh resin of the second CFRP part is infiltrated on top of the partially cross-linked CFRP surfaces. Afterwards, the joined parts are cured together in the final curing step. During this final curing process, the final morphology of the interface region develops. One important factor for the morphology and the resulting mechanical properties of the interface is the glass transition temperature of the partially cross-linked resin plate, which allows or prevents a softening of the resin at the beginning of final cure. Additionally, changes of density and modulus of the partially cured and fresh resins are

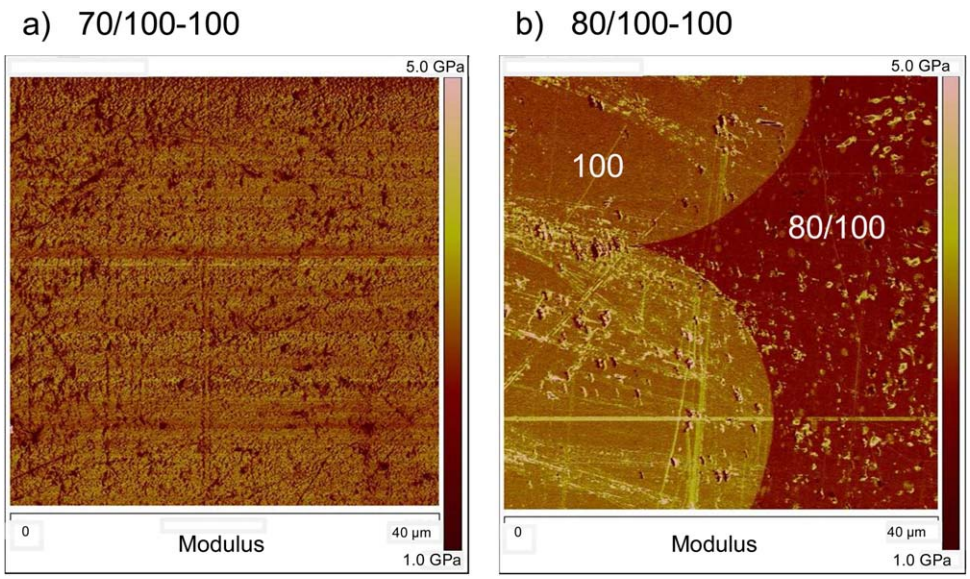

Figure 9. Scanning probe microscopy of interface region of (a) 70/100-100 and (b) 80/100-100 plate. [Color figure can be viewed in the online issue, which is available at wileyonlinelibrary.com.]

induced during the final curing cycle. These changes of material properties also influence the morphology of the joining region. A high mismatch of material properties will result in residual stresses and a significant inhomogeneity of the joining region.

If the glass transition temperature of the first, partially cross-linked plate is clearly below the final curing temperature, the partially cross-linked resin undergoes a transition into the rubber state and softens at the beginning of final curing. This applies to plates with cross-linking degrees of 60% and 70%. Their glass transition temperatures are measured as 77°C ± 2°C and 108°C ± 2°C, respectively. These are substantially lower than the final curing temperature of 180°C.[13] For these low cross-linking degrees a reasonable amount of unreacted polymer and hardener is still present. After softening, an intermixture of polymer and hardener molecules of the partially cross-linked and the fresh resin is possible. This allows a chemically controlled cross-linking of the first and the second CFRP plate. Additionally, material properties of the two joined resin parts after final cure are very similar. As shown in our previous work, density and modulus of 60/100 and 70/100 samples agree very well with those of completely cured 100 samples.[13] Scanning probe measurements of the cross-section of the 70/100-100 sample also show a homogeneous modulus distribution in the interface region [see Figure 9(a)]. Both findings contribute to a homogeneous resin morphology of the interface region of 60/100-100 and 70/100-100 samples, which is observed in Figure 10(a,b). The original surface of the partially cured plate cannot be located anymore. The resin interface area has a width of about 100 µm.

For plates with a curing degree of 80% and a glass transition temperature of 150°C ± 2°C the transition to the rubber state occurs at the beginning of final curing. However, as the glass transition temperature is close to the curing temperature, only a short period of softening exists. This likely allows only a limited intermixture and therefore favors inhomogeneous interface morphology. Consistently, in Figure 10(c) the original, ripple-like surface of the partially cured plate can be observed in the 50–100µm wide resin interface region. As analyzed by scanning probe measurements of the cross-section of a joined 80/100-100 sample [see Figure 9(b)] the different modulus values of the resins confirm the special nature of the interface region. Here also the ripple like peel-ply imprint is clearly observable. Significant differences in the AFM-modulus of the first plate (80/100) and the second plate (100) are measured in the interface region. The AFM-measurements are calibrated on the modulus value of a 100-ref sample of 2.89 GPa taken from literature.[23] The first plate (80/100) shows a clearly lower AFM-modulus of 2.34 GPa ± 0.2 GPa.

Also density measurements on partially cured pure resin agree with these results and show a significantly lower density of the finally cured 80/100 sample in comparison to the 100-ref sample.[24]

It should be noted, that previous nanoindentation modulus measurements on pure 80/100 and 100 resin samples did not show these clear differences of material properties.[13] Reason could be a confinement of the observed mismatch of resin moduli to the interface region of the joined samples. Possibly a surface hardening of the first, partially cured plate takes place before or during joining, which does not affect the bulk modulus of the sample.

The completely cured plate has a glass transition temperature of 209°C ± 2°C, which is significantly higher than the final curing temperature. Therefore, no transition to the rubber state and no softening can occur. Accordingly, after joining no mixture of resins and no cross-linking are possible. Our previous investigations on pure epoxy resin samples showed a clear density difference of the 100/100 sample and the 100 sample.[24] Nevertheless, no residues of the surface morphology of the partially cured plate are observable in the resin interface region in Figure

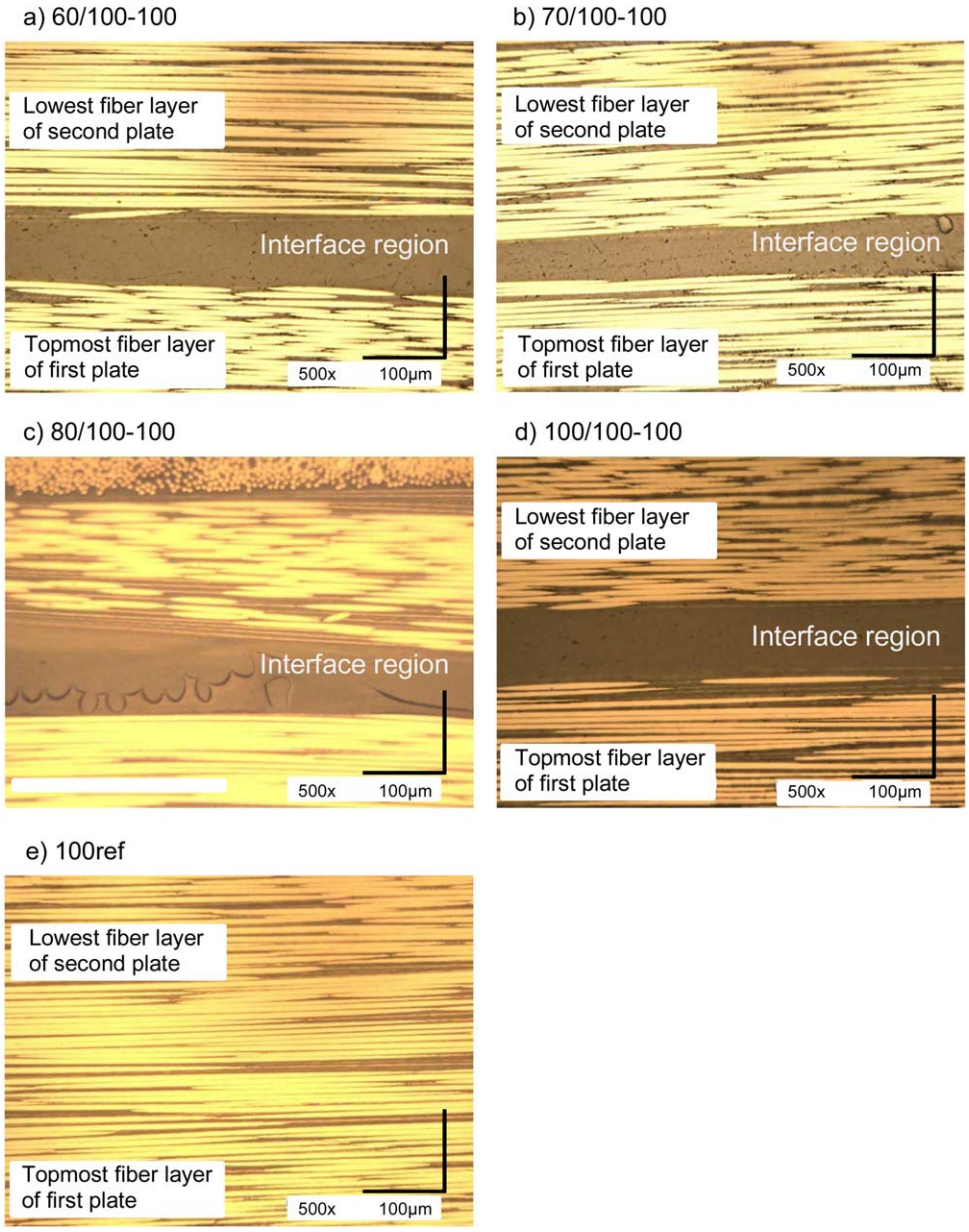

Figure 10. Cross sectional images of interface region of four types of joined samples: (a) 60/100-100 sample, (b) 70/100-100 sample, (c) 80/100-100 sample, (d) 100/100-100 sample, and (e) reference sample. [Color figure can be viewed in the online issue, which is available at wileyonlinelibrary.com.]

10(d). The about 100µm wide interface is characterized by a completely homogeneous resin morphology.

The completely cured reference sample shows no resin interface region at all [see Figure 10(e)]. Here the infiltration of the dry fiber layup is performed in one step. Therefore, no extended resin region exists between first and second fiber stacking.

The morphological properties of the interface region can be correlated to the observed bonding behavior, the fracture surface morphology and the surface morphology of the partially cured plate of the four types of joined plates and the reference sample.

For the reference sample no resin interface is observed between the two fiber stacking sequences. The crack dominantly propagates within the unidirectional fiber layers, which result in a high interlaminar fracture toughness and continuous crack propagation.

Joined samples with low G_{Ic} values, namely the 100/100-100 and the 60/100-100 plates, are characterized by interface regions with homogeneous resin structure. Failure occurs mostly within these interface regions, as the fracture surfaces reveal dominant contributions of matrix cracking. The brittle matrix failure without significant crack deflection results in low fracture toughness, low acoustic emission activity and discontinuous crack propagation.

Joined samples with high G_{Ic} values, namely samples of type 80/100-100, show an extended interface region with the pronounced structure of the peel-ply imprint. The ripple-like

surface structure of the partially cured plate is conserved even during joining and can cause a kind of mechanical interlocking of the joined plates. Additionally, a significant mismatch of resin properties of the joined parts is found. Possibly the crack is deflected by the highly structured interface region in direction to the weaker resin side, namely the 80/100 part. As this resin region is typically smaller than the infiltrated fresh resin part [see Figure 10(b)], the crack also is deflected towards the fiber reinforcements. Here interlaminar splitting and fiber breakage can occur, which are highly energy absorbing effects and may result in the observed high fracture toughness, high acoustic emission intensity and quasi-continuous crack growth.

Samples of type 70/100-100 cannot clearly be classified according to the characteristics discussed above. High fracture toughness and a clear ripple-like imprint after peel-ply pull-off are found. However, no defined structures in the resin interface regions exist. Also the 80/100-100 samples with low G_{Ic} values do not match the scheme described above. Here clear structures in the interface region exist, which do not correlate to high fracture toughness. Possible reason for this non consistent behavior can be the intermediate range of curing degrees between 70% and 80%. Here the so called transition region is located, where the resin transforms from rubber to glassy state during curing and the resin properties change significantly.[13] Small changes in the curing degree can cause step-like changes in the material properties, possibly creating a kind of two-phase material state with one material state closer to the 60/100-100 and one state close to the 80/100-100 samples.

CONCLUSIONS

Joining of partially cross-linked and freshly infiltrated epoxy resin marks a promising way for production of CFRP components with a high integration level. Partial cross-linking of the first CFRP part retains a certain reactivity of the thermosetting resin, which is used for bonding to a second, freshly infiltrated CFRP part. A final curing step guarantees the complete cross-linking of the joined components. The direct bonding of CFRP parts of the same resin system avoids several problems of common CFRP joining methods, e.g., surface treatment, insertion of additional materials or the drilling of holes.

Knowledge of the mechanical properties and the failure mode of the joined partially cured samples are crucial to optimize this novel joining process. To this end the fracture toughness of the joined plates, the acoustic emission activity during mechanical testing and the morphology of the fracture surfaces are investigated as function of the partial curing degree of the first plate. Additionally, the morphology of the interface region of the joined plates was analyzed by microscopic methods. A significant dependence of fracture toughness and the failure mode on the partial curing degree is found. Also the morphology of the interface region is dependent on the partial curing degree and has influence on the joining properties of a partially cured and a fresh resin part.

A general correlation of discontinuous, low acoustic emission activity, discontinuous crack propagation, smooth, resin dominated fracture surfaces and low fracture toughness was observed. Plates of this type, namely the samples 60/100-100 and 100/100-100, are further characterized by a relatively smooth resin surface of the partially cured plate after peel-ply pull-off and a homogeneous resin interface region. The crack propagation is dominantly observed in the resin rich area between the two joined plates, which is responsible for the poor bonding quality.

In contrast, intensive acoustic emission activity, quasi-continuous crack propagation and a fiber dominated crack surface structure are correlated to high fracture toughness values. Here intermediate curing degrees of 70 and 80% were found to be promising. The onset and mean fracture toughness of samples of type 70/100-100 and 80/100-100 is even higher than that of the reference sample, which represents the interlaminar fracture toughness of a completely cured CFRP plate in a conventional process. Often these samples types are characterized by a ripple-like surface morphology of the partially cured plate after peel-ply pull-off, which demonstrates a high contact surface and the possibility of mechanical interlocking. For the 80/100-100 samples the ripple-like structure is conserved even after final curing, resulting in an inhomogeneous interface morphology with significant differences in the material properties. The special combination of remaining chemical reactivity, high effective contact surface and mismatch of resin properties seems to be advantageous for the enhanced fracture toughness and the improved failure mode of the samples with partial curing degrees of the first plates of 70 and 80%.

The results demonstrate the outstanding options of joining of partially cured and freshly infiltrated CFRP laminates and proof the high potential of this novel method for direct bonding of CFRP components.

ACKNOWLEDGMENTS

Thanks to Jan Jäger for AFM investigation of the interface region of the joined samples.

REFERENCES

1. May, C. A. Epoxy Resins: Chemistry and Technology, 2nd ed.; New York: Marcel Dekker, **1988**.
2. Mohan, P. *Polym.-Plast. Technol. Eng.* **2013**, *52*, 107.
3. Guadagno, L.; Raimondo, M.; Vittoria, V.; Vertuccio, L.; Naddeo, C.; Russo, S.; De Vivo, B.; Lamberti, P.; Spinelli, G.; Tucci, V. *RSC Adv.* **2014**, *4*, 15474.
4. Bénard, Q.; Fois, M.; Grisel, M. *Int. J. Adhes. Adhes.* **2005**, *25*, 404.
5. Amancio-Filho, S. T.; dos Santos, J. F. *Polym. Eng. Sci.* **2009**, 1461.
6. Chukalovskaya, T. V.; Shcherbakov, A. I.; Chigirinskaya, L. A.; Bandurkin, V. V.; Medova, I. L.; Chukalovskii, P. A. *Prot. Met. Phys. Chem. Surf.* **1995**, *31*, 136.
7. Tavakkolizadeh, M.; Saadatmanesh, H. *J. Compos. Constr.* **2001**, August, 200.
8. Baldan, A. *Int. J. Adhes. Adhes.* **2012**, *38*, 95.
9. Fourche, G. *Polym. Eng. Sci.* **1995**, *35*, 957.

10. Gude, M. R.; Prolongo, S. G.; Urena, A. *Surf. Coat. Techn.* **2012**, *207*, 602.
11. Kanerva, M.; Saarela, O. *Int. J. Adhes. Adhes.* **2013**, *43*, 60.
12. Sause, M.; Llopard Prieto, L.; Scholler, J.; Horn, S.; Moosburger-Will, J.; Horny, R. Patent DE 10 2011 010 384 A1.
13. Moosburger-Will, J.; Greisel, M.; Sause, M. R.; Horny, R.; Horn, R. *J. Appl. Polym. Sci.* **2013**, *130*, 4338.
14. Bohse, J.; Krietsch, T.; Chen, J. H.; Brunner, A. J. In Fracture of Polymers, Composites and Adhesives; Williams, J. G., Pavan, A., Ed. Amsterdam: Elsevier Science, **2000**; Vol. *27*, p 15.
15. Bohse, J.; Chen, J. *J. Acoust. Emission.* **2001**, *19*, 1.
16. Sause, M. G. R.; Müller, T.; Horoschenkoff, A.; Horn, S. *Compos. Sci. Technol.* **2012**, *72*, 167.
17. Kostopoulos, V.; Tsotra, P.; Karapappas, P.; Tsantzalis, S.; Vavouliotis, A.; Loutas, T. H.; Paipetis, A.; Friedrich, K.; Tanimoto, T. *Compos. Sci. Technol.* **2007**, *67*, 822.
18. Kostopoulos, V.; Karapappas, P.; Loutas, T.; Vavouliotis, A.; Paipetis, A.; Tsotra, P. *Strain* **2011**, *47*, e269.
19. Toho. Toho Tenax Europe GmbH. Product literature to Tenax® HTA 40.
20. Hexcel. Hexcel Company. Product literature to HexFlow RTM6®.
21. Moosburger-Will, J.; Jäger, J.; Horn, S.; Wellhausen, C. *Polym. Test.* **2012**, *31*, 1008.
22. Sause, M. Dissertation, Identification of failure mechanisms in hybrid materials using pattern recognition techniques applied to acoustic emission signals. Berlin: Mensch und Buch Verlag: **2010**. ISBN: 978-3-86664-889-0.
23. Brauner, C.; Block, T. B.; Purol, H.; Herrmann, A. S. *J. Compos. Mater.* **2012**, *46*, 993.
24. Moosburger-Will, J.; Greisel, M.; Sause, M. G. R.; Horny, R.; Horn, S. *ECCM16.* **2014**.